Mode-selective internal conversion of perylene

Yoshitake Suganuma[a], Yasuyuki Kowaka[a], Noritaka Ashizawa[a], Naofumi Nakayama[b], Hitoshi Goto[c], Takayoshi Ishimoto[d], Umpei Nagashima[e,f], Tadashi Ueda[g], Takaya Yamanaka[g], Nobuyuki Nishi[g] and Masaaki Baba[a*]

[a]Division of Chemistry, Graduate School of Science, Kyoto University, Sakyo-ku, Kyoto 606-8502, Japan, [b]Conflex Corporation, 2-15-19 Kami-osaki, Shinagawa-ku, Tokyo 141-0021, Japan, [c]Department of Knowledge-based Information Engineering, Toyohashi University of Technology, Tempaku-cho, Toyohashi 441-8580, Japan, [d]INAMORI Frontier Research Center, Kyushu University, Motooka 744, Nishi-ku, Fukuoka 819-0395, Japan, [e]Research Institute for Computational Sciences, National Institute of Advanced Industrial Science and Technology, Umezono 1-1-1, Tsukuba, Ibaraki 305-8561, Japan, [f]Core Research for Evolutional Science and Technology, Japan Science and Technology Agency, 4-1-8 Honcho, Kawaguchi 332-0012, Japan, [g]Institute for Molecular Science, Myodaiji, Okazaki 444-8585, Japan

We observed fluorescence excitation spectra and dispersed fluorescence spectra for single vibronic level excitation of jet-cooled perylene-h_{12} and perylene-d_{12}, and carefully examined the vibrational structure of the S_0 ^1A_g and S_1 $^1B_{2u}$ states. We performed vibronic assignments on the basis of the results of ab initio calculation, and found that the vibrational energies in the S_1 state are very similar to those in the S_0 state, indicating that the potential energy curves are not changed much upon electronic excitation. We conclude that the small structural change is the main cause of its slow radiationless transition and high fluorescence quantum yield at the zero-vibrational level in the S_1 state. It has been already reported that the lifetime of perylene is remarkably short at specific vibrational levels in the S_1 state. Here, we show that the mode-selective nonradiative process is internal conversion (IC) to the S_1 state, and the $\nu_{16}(a_g)$

in-plane ring deforming vibration is the promoting (doorway) mode in the S_1 state which enhances vibronic coupling with the high-vibrational level (b_{2u}) of the S_0 state.

Keywords: perylene; vibrational structure; internal conversion; mode selectivity; ab initio calculation

*Correspondence author. E-mail: baba@kuchem.kyoto-u.ac.jp.

1. Introduction

Perylene is one of the prototypical large polycyclic aromatic hydrocarbons (PAHs) and has been the subject of extensive spectroscopic studies in condensed media and cold matrix.[1–5] It shows strong absorption in the violet and ultraviolet regions as well as strong fluorescence. The high fluorescence quantum yield is curious, because nonradiative relaxation is expected to be fast in a large polyatomic molecule due to its high density of coupling levels. Further, the perylene molecule does not conform to Hückel's rule, and its molecular structure is considered to be easily distorted. Radiationless transitions are generally enhanced by structural flexibility. Clearly, we stand to learn much through investigating the isolated molecule. There have also been extensive studies on jet-cooled perylene[6–10]; These experimental results demonstrated that the fluorescence quantum yield was high, and that radiationless transitions such as predissociation, intersystem crossing (ISC) to the triplet state, and internal conversion (IC) to the S_0 state, were all slow in the S_1 state even for the isolated perylene molecule.

We have recently shown through a rotational analysis that the S_1 state is $^1B_{2u}$ and is approximately expressed by the configuration of HOMO $\rightarrow$ LUMO one-electron excitation, and that the slow nonradiative processes can be attributed to the fact that structural change occurs on such a small scale upon $S_1 \leftarrow S_0$ electronic excitation.[11] It is still necessary to investigate the potential energy curves or vibrational energies in both the S_0 and S_1 states. As shown below, a theoretical approach predicts that the probable nonradiative process is IC to the S_0 state. If the potential energy curves of the S_0 and S_1 states are identical, the IC rate in the S_1 state is zero because the vibrational overlap between the S_1 zero-vibrational level and S_0 high-vibrational levels is vanishing. Kaziska et al. found that the fluorescence lifetime was remarkably short in specific vibrational levels of the S_1 state.[8] The lifetimes were reported to be 8.88, 3.54, 1.46, and 0.38 ns for excitations of the 0, 353, 705, and 900 cm^{-1} bands, respectively. It indicates that the radiationless transition is selective for a specific vibrational mode. We observed fluorescence excitation spectra and dispersed fluorescence

spectra of the $S_1 \leftrightarrow S_0$ transitions of jet-cooled perylene-h_{12} and perylene-d_{12}, and carefully analyzed their vibronic structures in the S_0 and S_1 states on the basis of ab initio theoretical calculation. In this article, we present the results of these jet spectroscopy experiments and ab initio calculations, and discuss the structure and excited-state dynamics in the S_1 $^1B_{2u}$ state of the isolated perylene molecule.

2. Experiment

Commercially obtained perylene-h_{12} and perylene-d_{12} (Wako Chemical, 98%) were used without further purification. The solid sample was heated to 150°C in a stainless steel container. The vapor was mixed with Ar gas and expanded into a vacuum chamber through a pulsed nozzle (an automobile fuel injector) to generate a supersonic jet. The jet was crossed with a pulsed laser beam at right angles. As a light source, we employed a tunable dye laser (Lambda Physik LPD 3002, $\Delta E = 0.1$ cm^{-1}, Exalite 398 and 416) pumped by an excimer laser (Coherent Compex Pro 110, 308 nm, 200 mJ). The laser beam was focused to 3 mm^2 by a lens, and the pulse energy was reduced to less than 1 mJ to avoid saturation. Fluorescence from the excited molecules was collected using a lens to a photomultiplier tube (Hamamatsu R928), of which the output was processed using a boxcar integrator (Stanford Research SR200). The change in fluorescence intensity in response to the laser wavelength was recorded as a fluorescence excitation spectrum using the LabView system. The output power of the dye laser changed with wavelength more than twice, so that the fluorescence intensity was normalized by the laser power. A dispersed fluorescence spectrum was observed using a scanning monochromator (Nikon P250).

3. Results and Discussion

The molecular structure of perylene and its coordinate axes are illustrated in Figure 1. The aromatic stability of a PAH molecule is predicted by Hückel's

$4n + 2$ rule, which states that cyclic planar molecules in which each atom has a p orbital are aromatic if they contain $4n + 2$ π electrons. Perylene possesses 20 π electrons and does not have any aromatic stabilization. We have, however, demonstrated that the isolated perylene molecule is planar (D_{2h} symmetry) in its S_0 and S_1 states by experimentally obtaining its rotational constants.[11] All three axes possess a two-fold axis (C_2) and two mirror planes (σ_h) and (σ_v) although the rotational constant values are all different (an asymmetric top). The axis notation is, therefore, important to express the electronic and vibrational irreducible representations distinctly. Here, we assign the x and y axes to the in-plane short and long axes, respectively. The z axis is perpendicular to the molecular plane. Although this notation is different from the conventional one, it is convenient for the expression of electronic transition and is consistent with linear polyacenes such as naphthalene and anthracene. The y axis is parallel to the center C=C double bonds. The S_1 state of perylene is represented as $^1B_{2u}$. The transition moment is large along this direction and the $S_1 \leftarrow S_0$ transition is strong, which is identified as ^1L_a.[12] Fluorescence excitation spectra of the S_1 $^1B_{2u}$ $\leftarrow$ S_0 ^1A_g transition of perylene-h_{12} and perylene-d_{12} in supersonic jets are shown in Figure 2. The vibrational energies of observed vibronic bands are listed in Table 1. The 0_0^0 band (24059 cm^{-1}, 415.53 nm) is very strong, suggesting that the structural change upon $S_1 \leftarrow S_0$ electronic excitation. Surprisingly, the transition wavenumber of the 0_0^0 band of perylene-d_{12} was identical to that of perylene-h_{12}. A number of low-frequency bands appeared when we reduced the stagnation pressure of Ar gas and raised the vibrational temperature of the supersonic jet. The observed spectrum was similar to the cavity ringdown spectrum, for which the vibronic assignments are almost complete.[9] The prominent vibronic bands are assigned to totally symmetric a_g bands.[7] The newly appearing bands represent the transitions between vibrational energy levels of out-of-plane ring torsion ν_{52} (a_u), butterfly ν_{60} (b_{1u}), and in-plane ring deforming ν_{75} (b_{2u}) modes, for instance, 52_n^n, $52_n^n 75_1^1$, $16_0^1 75_n^n$, and so on. The assignments and shifts from the 0_0^0 band are tabulated in Table 2. These are *ungerade* vibrations in which the fundamental bands are forbidden, whereas the overtone and hot bands are allowed. In order

to investigate the vibrational structure in the S_0 state, we observed dispersed fluorescence spectra tuning the laser wavelength to each 0_0^0 band of perylene-h_{12} and perylene-d_{12}. The results are shown in Figure 3, and the vibrational energies of observed bands are listed in Table 3. The prominent vibronic bands are assigned to the transitions of the a_g vibrational levels in the same manner as the excitation spectrum.

We analyzed these spectroscopic results with the assistance of ab initio theoretical calculation using the Gaussian 09 program package.[13] The S_1 state has been identified as $^1B_{2u}$ through an analysis of selection rules for rotational transitions. The $S_1 \leftarrow S_0$ absorption is an allowed strong transition of which the moment is parallel to the long (y) axis. Ab initio calculation of vibrational energies is required to analyze the vibronic structure. We examined several methods of calculation in order to identify the one which yielded rotational constant values closest to those obtained experimentally. We then calculated the normal vibrational energies with the optimized geometrical structure.

The rotational constants in the S_0 ^1A_g state of perylene-h_{12} have been reported as A =0.021132, B =0.0111077, and C =0.0072744 cm^{-1}.[11] We have shown that the RHF/6-311+G(d,p) calculation yields A =0.021113, B =0.011106, and C =0.0072775 cm^{-1}. The difference between the experimental and calculated values is only 0.09% for the A value. The calculated x and y coordinates of each atom are tabulated in Table 4. The calculated vibrational energies exhibit good conformity with the observed vibrational energies in the dispersed fluorescence spectrum using a scaling factor of 0.955, which has been determined by a least-squares fit of the observed vibrational energies. The resultant values are listed in Table 5 together with the experimental values. The assignments of vibronic bands are also shown in Table 3. The vibrational energies calculated using the Gaussian 09 program provides the harmonic energies, and the 5% reducing factor might be due to an anharmonic effect. The fundamental bands observed in the spectrum are all shown to occur due to the a_g mode. The assignments of perylene-h_{12} are reliable because the vibrational energies are in fairly good agreement with the calculated ones. Although the a_g C-H stretch band is forbidden for the

infrared absorption, a strong b_{2u} or b_{3u} band was observed at 3065 cm^{-1} through infrared cavity ringdown spectroscopy.[14] Our calculated value is 3074 or 3076 cm^{-1}, which is also in good agreement with this experimental value. In general, many normal mode energies are remarkably reduced by deuterium substitution in PAH molecules.[15,16] The observed vibrational energies of perylene-d_{12} are also in good agreement with the calculated ones with the identical structure and scaling factor.

The rotational constants in the S_1 $^1B_{2u}$ state are A =0.020847, B =0.0112638, and C =0.0073044 cm^{-1}, which are not much different from those in the S_0 state. Typically, rotational constants in the S_1 state are slightly smaller than those in the S_0 state because the antibonding character increases upon $\pi\pi^\star$ electronic excitation. In the perylene molecule, however, the changes in rotational constants are very small and the B and C values in the S_1 state are rather greater than that in the S_0 state. By the RCIS/6-31+G(d,p) method, we obtained A =0.020783, B =0.011252, and C =0.0073000 cm^{-1} values, which are in good coincidence with the experimental values. The difference is only 0.3% for the A value. The calculated vibrational energies in the S_1 state, which were scaled by a factor of 0.918, were in good agreement with the excess energies of vibronic bands observed in the fluorescence excitation spectrum. The resultant values are listed in Table 5. On the basis of these results of ab initio calculation, we assigned the vibronic bands as shown in Tables 1 and 2. We conclude that the stable equilibrium structure and potential energy curves of perylene are not changed much by $S_1 \leftarrow S_0$ electronic excitation. The change in each bond order resulting from the HOMO $\rightarrow$ LUMO electronic excitation is expected to be small, because the π wavefunction is uniformly distributed over the whole molecule, and the changes are diluted with a large number of π electrons. This feature is considered to be common to large PAH molecules.

We discuss here the radiationless transition in the S_1 state of perylene. If the equilibrium structure and potential energy curves are similar between the S_0 and S_1 states, it is generally expected that fluorescence lifetime is long and quantum yield is high. The fluorescence lifetime at the zero-vibrational level in the S_1

state of perylene is 8.88 ns,[8] and the fluorescence quantum yield is almost unity.[9] These facts indicate that radiationless transitions such as predissociation, ISC to the triplet state, and IC to the S_0 state are all slow in the isolated perylene molecule. The bond energies are much larger than the $S_1 \leftarrow S_0$ excitation energy, and predissociation is not expected to occur in the S_1 state. The ISC to the triplet state is theoretically considered to be slow by El-Sayed's rule that spin-orbit interaction between the $^1\pi\pi^\star$ and $^3\pi\pi^\star$ is weak for a planar molecule.[17] It has been experimentally confirmed by means of magnetic moment measurement using ultrahigh-resolution Zeeman spectroscopy for benzene,[18,19] naphthalene,[20,21] anthracene,[15] pyrene,[16] and perylene itself.[11] The Zeeman splitting in the external magnetic field was found to be very small. The Hamiltonian for spin-orbit interaction is expressed as[22]

$$H_{SO} = \frac{e^2}{2m^2c^2} \sum_i^n \sum_k^m \frac{Z_k(\boldsymbol{r}_{ik} \times \boldsymbol{p}_i) \cdot \boldsymbol{s}_i}{{r_{ik}}^3} , \tag{1}$$

and can be written for each electron as

$$\frac{e^2}{2m^2c^2} \left[\left(\sum_k^m \frac{Z_k \boldsymbol{l}_{xk}}{{r_k}^3} \right) \boldsymbol{s}_x + \left(\sum_k^m \frac{Z_k \boldsymbol{l}_{yk}}{{r_k}^3} \right) \boldsymbol{s}_y + \left(\sum_k^m \frac{Z_k \boldsymbol{l}_{zk}}{{r_k}^3} \right) \boldsymbol{s}_z \right] , \tag{2}$$

since $\boldsymbol{s}_i$ is independent of space coordinates. For the $\pi\pi^\star$ state composed of $2p_z$ atomic orbitals, the nonzero element arises from the operator H_z, which is expressed in the form

$$\frac{ie^2h^2}{4m^2c^2} \frac{Z}{{r_k}^3} \left[(x - x_k^0) \frac{\partial}{\partial y} - (y - y_k^0) \frac{\partial}{\partial x} \right] . \tag{3}$$

The spin-orbit matrix element is vanishing for the S_1 and T_1 states of the same symmetry (the same irreducible representation). Even in different configurations, the one- and two-center integrals are vanishing between the $^1\pi\pi^\star$ and $^3\pi\pi^\star$ states. In contrast, large Zeeman broadening and shifts of the rotational lines by the external magnetic field were observed in pyrazine[23] and glyoxal,[24] in which the $S_1(^1n\pi^\star)$ and $T_2(^3\pi\pi^\star)$ states are close in energy. In perylene, however, it has been shown that the singlet-triplet interaction is very weak and that the ISC is very slow at the S_1 zero-vibrational level.[11] Zeeman broadening of rotational

lines was actually observed in benzene, naphthalene, and anthracene, in which the magnetic moment is induced by $J-L$ interaction (L-uncoupling interaction) between the $^1B_{2u}$ and $^1B_{3u}$ states, and the magnitude of Zeeman broadening is given by

$$\mathrm{ZS}(\mathrm{S}_1\ {}^1B_{2u}\ vJK_c) \ = \ \frac{8CK_c^2}{J+1}\frac{|<\mathrm{S}_2\ {}^1B_{3u}|L_y|\mathrm{S}_1\ {}^1B_{2u}>|^2}{E(\mathrm{S}_2)-E(\mathrm{S}_1)}\mu_B H\ . \tag{4}$$

The actual broadening was found to be on the order of 0.005 cm^{-1} at 0.5 Tesla for the $J=K_c=40$ level in anthracene. In perylene, the broadening is expected to be much smaller than this, because of its smaller rotational constants and larger energy difference between the $^1B_{2u}$ and $^1B_{3u}$ states.

The IC at the S_1 zero-vibrational level is caused by vibronic interaction with the S_0 high-vibrational levels. The IC rate at a vibronic level of the S_1 state is represented as[25–27]

$$\begin{aligned} W_{IC} \quad &\propto \quad \sum_i \left|\left\langle \phi_{\mathrm{S}_0}\left|\frac{\partial}{\partial Q_i}\right|\phi_{\mathrm{S}_1}\right\rangle\right|^2 \ \left|\left\langle \chi_{\mathrm{S}_0}^{v''}\left|\frac{\partial}{\partial Q_i}\right|\chi_{\mathrm{S}_1}^{v'}\right\rangle\right|^2 \ \delta(E_{\mathrm{S}_1}^{v'}-E_{\mathrm{S}_0}^{v''}) \\ &\approx \quad \frac{\sum_i \left|\left\langle \phi_{\mathrm{S}_0}(r,Q_0)\left|\left(\frac{\partial U(r,Q)}{\partial Q_i}\right)_{Q_0}\right|\phi_{\mathrm{S}_1}(r,Q_0)\right\rangle\right|^2}{(E_{\mathrm{S}_1}(Q_0)-E_{\mathrm{S}_0}(Q_0))^2} \\ &\quad \times \left|\left\langle \chi_{\mathrm{S}_0}^{v''}(Q_i)\left|\frac{\partial}{\partial Q_i}\right|\chi_{\mathrm{S}_1}^{v'}(Q_i)\right\rangle \prod_{j\neq i}\left\langle \chi_{\mathrm{S}_0}^{v''}(Q_j)|\chi_{\mathrm{S}_1}^{v'}(Q_j)\right\rangle\right|^2 \\ &\quad \times \delta(E_{\mathrm{S}_1}^{v'}-E_{\mathrm{S}_0}^{v''})\ . \end{aligned} \tag{5}$$

Here, ϕ_{S_0} and ϕ_{S_1} represent the electronic wavefunctions of the S_0 and S_1 states, respectively. $\chi_{\mathrm{S}_0}^{v''}$ is the vibrational wavefunction of the high-vibrational level in the S_0 state, and $\chi_{\mathrm{S}_1}^{v'}$ is that of the vibrational level in the S_1 state. δ is the Dirac delta function, and Q_i is a normal coordinate. The second and third matrix elements are the adiabatic Franck-Condon factor for a promoting mode (i) and the Franck-Condon factor of other modes (j) , respectively. Although the S_0 and S_1 states are coupled by a b_{2u} vibration, these vibrational overlaps are vanishing when the potential energy curves are identical for the S_0 and S_1 states. There are two situations that can induce enhancement: one of these is change

in the equilibrium molecular structure (displacement). The edge of the potential curve approaches that for the S_1 state, so that the overlap of wavefunctions becomes larger. Yet the experimentally determined rotational constants at the zero-vibrational level of the S_1 state are very similar to those of the S_0 state[11]; consequently, the displacement in the perylene molecule is considered to be very small. The other situation that can induce enhancement is change in the slope of the potential energy curve (distortion). We have demonstrated in the present work that the vibrational energies of the S_0 and S_1 states are very similar in the perylene molecule. This observation indicates that the distortion is very small. Eventually, all radiationless transitions in the perylene molecule are considered to be slow due to the small scale of change in the molecular structure and potential energy curve. This is similar to the situation in the pyrene molecule, which possesses 16 π electrons rather than the stable aromatic system of Hückel's rule.[15] The fluorescence lifetime of pyrene (1400 ns) is much longer than that of perylene (8.88 ns).[27] Pyrene's long lifetime is due to its radiative lifetime, because the S_1 state is ${}^1B_{3u}({}^1L_b)$ and the $S_1 \leftarrow S_0$ transition moment is small.[12] The radiationless transitions are remarkably slower than the radiative transition and the fluorescence quantum yield is high.

In perylene, a number of low-frequency normal modes exist; this feature makes perylene unique among PAH molecules. The four normal vibrational modes, shown in Figure 4, are important for radiative and nonradiative processes in the S_1 state. The fundamental vibrational energy of ν_{52} (a_u) is the smallest in any of the 90 normal modes. The major change in this vibration occurs in the bond angles around the C(4)-C(5) bond. The C(4)-C(5) bond order increases upon $S_1 \leftarrow S_0$ excitation. Consequently, the shape of the potential energy curve differs between the S_0 and S_1 states. The large intensity of the 52_n^{n+2} hot bands strongly suggests this significant change in the potential energy curves. The slope in the S_1 state is, however, rather steeper than that in the S_0 state, so that the vibrational overlap between the S_1 zero-vibrational level and S_0 high-vibrational levels is expected to be small. This mode is not considered to be important in the IC process in the S_0 state.

Another out-of-plane vibration in the symmetric phase is the ν_{60} (b_{1u}) butterfly mode. The fundamental energy is slightly reduced in the S_1 state, and the vibrational overlap between the S_0 high-vibrational levels is expected to be larger. These two out-of-plane modes are radiatively active for the two-quanta transition and hot bands, but is impossible for either of them to be a promoting mode of vibronic coupling between the S_0 and S_1 states because they are coupled by the b_{2u} vibration.

Next, we consider a few of the in-plane modes which are important for the IC in the S_1 state of perylene. It has been reported that the fluorescence lifetime is remarkably short at the 16^1, 16^2, and $14^1 16^1$ levels,[8] and this indicates that the ν_{16} (a_g) mode is a promoting (doorway) mode of vibronic coupling in the S_1 state. As shown in Figure 3(c), all of the C atoms move mainly in the direction of the molecular long axis (y). The vibrational energy is relatively small because this mode is mainly represented by the change of bond angles. The observed energy of the S_1 state, however, is almost identical to that of the S_0 state, indicating that the shapes of the potential energy curves of these two electronic states are similar. It is supposed, however, that the stable geometrical structure is slightly different with respect to this normal coordinate. The experimentally determined rotational constants suggest that the molecule shrinks and expands along its long and short molecular axes, respectively. This structural change is also suggested by the relatively strong intensity of the 16_0^1 and 16_0^2 bands in the fluorescence excitation spectrum.

The ν_{75} (b_{2u}) mode is another in-plane ring deforming vibration in the antisymmetric phase. The C atoms also move mainly in the y direction, whereas the C-H bonds oscillating in the x direction. Any (b_{2u}) modes are potential promoting modes of vibronic coupling between the S_0 ^1A_g and S_1 $^1B_{2u}$ states. In particular, the ν_{75} mode, which is the b_{2u} mode with the least energy, is considered to be the most important vibration for the IC process in the S_1 state because the ν_{16} (a_g) mode is the promoting (doorway) vibration in which the C atoms mainly move along the long molecular axis (y). Thus, it is concluded that the IC in the S_1 state of perylene is enhanced mainly by the in-plane vibrational motion along the

long molecular axis with the promoting mode of ν_{75} (b_{2u}) in the S_0 state and the promoting (doorway) mode of ν_{16} (a_g) in the S_1 state.

In these in-plane deforming vibrations, the energy is small and the displacement is large. The structural change resulting from zero-point vibration is, therefore, sufficiently large to provide effective moments of inertia which are greater than the moments of inertia of a frozen molecule.[29,30] As a result, the rotational constants at the zero-vibrational level are altered to give a nonzero value of inertial defect, which is zero for a frozen planar molecule. Large planar molecules generally exhibits negative inertial defects[31]; the perylene molecule, in contrast, exhibits a positive inertial defect, suggesting that the in-plane vibrations have an important influence on the averaged molecular structure over zero-point vibration.[11] If the molecule is distorted out-of-plane, or if out-of-plane vibration makes a large contribution to the effective moment of inertia, the value of the inertial defect becomes negative and appreciably large. The perylene molecule is, therefore, considered to be planar and the low-frequency out-of-plane modes such as ring torsion and butterfly are not considered to be important for the inertial defect.

4. Summary

We observed fluorescence excitation spectra and dispersed fluorescence spectra of the $S_1 \leftarrow S_0$ transition of jet-cooled perylene-h_{12} and perylene-d_{12}. We assigned vibronic bands to their corresponding transitions using the reliable results of ab initio theoretical calculation, which yielded rotational constant values approximately equal to those obtained experimentally. We employed RHF/6-311+G(d,p) and RCIS/6-31+G(d,p) for the S_0 ^1A_g and S_1 $^1B_{2u}$ states, respectively. The observed vibrational energies of the S_0 and S_1 states of perylene-h_{12} are in good agreement with the calculated vibrational energies using scaling factors of 0.955 and 0.918, respectively.

We conclude that, in perylene, the molecular structure and potential energy curves are approximately identical for the S_0 and S_1 states. The extremely small

deuterium shift of the $S_1 \leftarrow S_0$ 0_0^0 band also indicates that the vibrational energies for the S_0 and S_1 states are almost identical as well. The slow IC process and high fluorescence quantum yield in the S_1 state are attributed to the small scale of the structural change that occurs upon electronic excitation. The abnormally short lifetime in the vibrational levels concerned with the $\nu_{16}(a_g)$ ring-deforming normal mode is attributed to strong vibronic interaction with the high-vibrational levels in the S_0 state. The IC process is remarkably enhanced by this promoting (doorway) mode in the S_1 state and the b_{2u} promoting modes in the S_0 state.

Acknowledgement

This work was supported by the Joint Studies Program (2010-2011) of the Institute for Molecular Science. The experiment was supported by the Inter-University Network for Efficient Utilization of Chemical Research Equipments. This research was also supported by a Grant-in-Aid for the Global COE Program, "International Center for Integrated Research and Advanced Education in Materials Science", from the Ministry of Education, Culture, Sports, Science and Technology of Japan.

References

[1] M. Lamotte, A. M. Merle, J. Joussot-Dubien, and F. Dupuy, Chem. Phys. Lett. **35**, 410 (1975).

[2] I. I. Abram, R. A. Auerbach, R. R. Biege, B. E. Kohler, and J. M. Stevenson, J. Chem. Phys. **63**, 2473 (1975).

[3] J. Olmsted, III, J. Phys. Chem. **83**, 2581 (1979).

[4] C. Joblin, F. Salama, and L. Allamandola, J. Chem. Phys. **110**, 7287 (1999).

[5] T. M. Halasinski, J. L. Weisman, R. Ruiterkamp, T. J. Lee, F. Salama, and M. Head-Gordon, J. Phys. Chem. A **107**, 3660 (2003).

[6] B. E. Forch, K. T. Chen, and E. C. Lim, Chem. Phys. Lett. **100**, 389 (1983).

[7] S. A. Schwartz and M. R. Topp, Chem. Phys. **86**, 245 (1984).

[8] A. J. Kaziska, S. A. Wittmeyer, A. L. Motyka, and M. R. Topp, Chem. Phys. Lett. **154**, 199 (1989).

[9] M. Sonnenschein, A. Amirav, and J. Jortner, J. Phys. Chem. **88**, 4214 (1984).

[10] X. Tan and F. Salama, J. Chem. Phys. **122**, 084318 (2005).

[11] Y. Kowaka, Y. Suganuma, N. Ashizawa, N. Nakayama, H. Goto, T. Ishimoto, U. Nagashima, and M. Baba, J. Mol. Spectrosc. **260**, 72 (2010).

[12] H. B. Klevens and J. R. Platt, J. Chem. Phys. **17**, 470 (1949).

[13] Revision *A.02*, M. J. Frisch, G. W. Trucks, H. B. Schlegel, G. E. Scuseria, M. A. Robb, J. R. Cheeseman, G. Scalmani, V. Barone, B. Mennucci, G. A. Petersson, H. Nakatsuji, M. Caricato, X. Li, H. P. Hratchian, A. F. Izmaylov, J. Bloino, G. Zheng, J. L. Sonnenberg, M. Hada, M. Ehara, K. Toyota, R. Fukuda, J. Hasegawa, M. Ishida, T. Nakajima, Y. Honda, O. Kitao, H. Nakai, T. Vreven, J. A. Montgomery, Jr., J. E. Peralta, F. Ogliaro, M. Bearpark,

J. J. Heyd, E. Brothers, K. N. Kudin, V. N. Staroverov, R. Kobayashi, J. Normand, K. Raghavachari, A. Rendell, J. C. Burant, S. S. Iyengar, J. Tomasi, M. Cossi, N. Rega, J. M. Millam, M. Klene, J. E. Knox, J. B. Cross, V. Bakken, C. Adamo, J. Jaramillo, R. Gomperts, R. E. Stratmann, O. Yazyev, A. J. Austin, R. Cammi, C. Pomelli, J. W. Ochterski, R. L. Martin, K. Morokuma, V. G. Zakrzewski, G. A. Voth, P. Salvador, J. J. Dannenberg, S. Dapprich, A. D. Daniels, O. Farkas, J. B. Foresman, J. V. Ortiz, J. Cioslowski, and D. J. Fox, Gaussian, Inc., Wallingford CT, 2009.

[14] A. J. Huneycutt, R. N. Casaes, B. J. McCall, C.-Y. Chung, Y.-P. Lee, and R. J. Saykally, ChemPhysChem **5**, 321 (2004).

[15] M. Baba, M. Saitoh, K. Taguma, K. Shinohara, K. Yoshida, Y. Semba, S. Kasahara, N. Nakayama, H. Goto, T. Ishimoto, and U. Nagashima, J. Chem. Phys. **130**, 134315 (2009).

[16] M. Baba, M. Saitoh, Y. Kowaka, K. Taguma, K. Yoshida, Y. Semba, S. Kasahara, Y. Ohshima, T. Yamanaka, Y.-C. Hsu, and S. H. Lin, J. Chem. Phys. **131**, 224318 (2009).

[17] M. A. El-Sayed, J. Chem. Phys. **38**, 2834 (1963).

[18] A. Doi, S. Kasahara, H. Katô, and M. Baba, J. Chem. Phys. **120**, 6439 (2004).

[19] J. Wang, A. Doi, K. Kasahara, H. Katô, and M. Baba, J. Chem. Phys. **121**, 9188 (2004).

[20] M. Okubo, J. Wang, M. Baba, M. Misono, S. Kasahara, and H. Katô, J. Chem. Phys. **122**, 144303 (2005).

[21] K. Yoshida, Y. Semba, S. Kasahara, T. Yamanaka, and M. Baba, J. Chem. Phys. **130**, 194304 (2009).

[22] D. S. McClure, J. Chem. Phys. **20**, 682 (1952).

[23] N. Yamamoto, T. Ebi, and M. Baba, J. Chem. Phys. **105**, 5745 (1996).

[24] H. Katô, K. Sawa, H. Kuwano, S. Kasahara, M. Baba, and S. Nagakura, J. Chem. Phys. **109**, 4798 (1998).

[25] S. H. Lin, J. Chem. Phys. **44**, 3759 (1966).

[26] W. Siebrand, J. Chem. Phys. **46**, 440 (1967).

[27] M. Bixon and J. Jortner, J. Chem. Phys. **48**, 715 (1968).

[28] E. A. Mangle and M. R. Topp, J. Phys. Chem. **90**, 802 (1986).

[29] D. R. Herschbach and V. W. Laurie, J. Chem. Phys. **37**, 1668 (1964).

[30] V. W. Laurie and D. R. Herschbach, J. Chem. Phys. **37**, 1687 (1964).

[31] T. Oka, J. Mol. Struct. **352/353**, 225 (1995).

Table 1. Vibrational energies (cm^{-1}) and assignments of the bands observed in the fluorescence excitation spectra of the $S_1\ ^1B_{2u} \leftarrow S_0\ ^1A_g$ transition of perylene-h_{12} and perylene-d_{12}. The accuracy is ± 1 cm^{-1}.

Vibrational energy		Assignment
h_{12}	d_{12}	
0	0	0_0^0 (24059 cm^{-1} both for h_{12} and d_{12})
75	72	
94	90	$52_0^2(a_u)$
164	155	
180	170	
193	183	$60_0^2(b_{1u})$
350	331	$16_0^1(a_g)$
424	401	$15_0^1(a_g)$
447	421	$16_0^1(a_g)52_0^2(a_u)$
547	515	$14_0^1(a_g)$
703	663	$16_0^2(a_g)$
777	732	$15_0^1(a_g)16_0^1(a_g)$
793	748	$13_0^1(a_g)$
898		$14_0^1(a_g)16_0^1(a_g)$
976	846	$12_0^1(a_g)$
1003		
1053	995	$16_0^3(a_g)$
1100		$11_0^1(a_g)$
1144		
1191		$10_0^1(a_g)$
1241		
1293		$9_0^1(a_g)$
1397	1293	$7_0^1(a_g)$
1553		$5_0^1(a_g)$
1601		
1644	1601	$4_0^1(a_g)$
1748		

Table 2. Assignment and shift (cm^{-1}) from the 0_0^0 band of the observed bands in the fluorescence excitation spectra of the $S_1\ ^1B_{2u} \leftarrow S_0\ ^1A_g$ transition of perylene-h_{12} and perylene-d_{12} at a higher vibrational temperature. The accuracy is ± 1 cm^{-1}.

Assignment	n	Shift (cm^{-1})	
		h_{12}	d_{12}
$75_n^n(b_{2u})$	0	0	0
	1	-9	-8
	2	-17	-15
$37_n^n(b_{2g})60_1^1(b_{1u})$	0	-11	-10
	1	-33	-31
	2	-53	-50
$52_n^n(a_u)75_1^1(b_{2u})$	0	-9	-8
	1	12	11
	2	32	31
	3	52	
	4	74	
$52_n^n(a_u)$	0	0	0
	1	22	21
	2	43	40
	3	62	59
	4	81	75
$52_n^{n+2}(a_u)$	0	95	90
	1	119	113
	2	141	134
	3	162	152
	4	181	171
	5	200	189
	6	218	
$16_0^1(a_g)75_n^n(b_{2u})$	0	350	331
	1	341	322
	2	333	314
$16_0^1(a_g)52_n^n(a_u)75_1^1(b_{2u})$	0	341	322
	1	363	343
	2	384	363
$16_0^1(a_g)52_n^n(a_u)$	0	350	331
	1	373	353
	2	393	371
	3	412	390
	4		407

Table 3. Vibrational energies (cm^{-1}) and assignments of the bands observed in the dispersed fluorescence spectra for excitation of the $S_1\ ^1B_{2u} \leftarrow S_0\ ^1A_g\ 0_0^0$ bands of perylene-h_{12} and perylene-d_{12}. The accuracy is ± 3 cm^{-1}.

Vibrational energy		Assignment
h_{12}	d_{12}	
0	0	0_0^0 (24059 cm^{-1} both for h_{12} and d_{12})
55	45	$52_2^0(a_u)$
361	337	$16_1^0(a_g)$
413		$16_1^0(a_g)52_2^0(a_u)$
438	401	$15_1^0(a_g)$
562	528	$14_1^0(a_g)$
722	675	$16_2^0(a_g)$
819	741	$13_1^0(a_g)$
926		$14_1^0(a_g)16_1^0(a_g)$
1083	1018	$16_3^0(a_g)$
1135	926	$11_1^0(a_g)$
1339	1102	$9_1^0(a_g)$
1413	1370	$7_1^0(a_g)$
1677	1603	$5_1^0(a_g)$
1773	1627	$4_1^0(a_g)$
1854	1786	
2081		
2167		
2240	1993	
2289		
2454	2352	
2766	2416	
2836		
2945	2830	
3017		
3095		
3171	3010	

Table 4. Calculated coordinates (Å) of each atom in the S_0 and S_1 states of perylene.

	$S_0\ {}^1A_g{}^a$		$S_1\ {}^1B_{2u}{}^b$	
	x	y	x	y
C(1)	1.2286	3.5577	1.2264	3.5394
C(2)	2.4021	2.8781	2.4241	2.8492
C(3)	2.4067	1.4706	2.4402	1.4674
C(4)	1.2468	0.7428	0.2368	0.7203
C(18)	0.0000	2.8541	0.0000	2.8484
C(19)	0.0000	1.4412	0.0000	1.4174
H(21)	1.2140	4.6831	1.2213	4.6151
H(22)	3.3390	3.4059	3.3538	3.3898
H(23)	3.3595	0.9801	3.3882	0.9697

[a] Calculated by RHF/6-311+G(d,p).
[b] Calculated by RCIS/6-31+G(d,p).

Table 5. Normal modes and vibrational energies (cm^{-1}) of perylene.

Symmetry	Number	Vibration type	$S_0\ ^1A_g$		$S_1\ ^1B_{2u}$	
			h_{12}	d_{12}	h_{12}	d_{12}
			Calc.[a] (Obs.)[b]	Calc.[a] (Obs.)[b]	Calc.[c] (Obs.)[d]	Calc.[c] (Obs.)[d]
a_g	1	C-H stretch	3237	2410	3151	2327
	2	C-H stretch	3194	2388	3094	2292
	3	C-H stretch	3173	2361	3076	2272
	4	C-C stretch + C-H wag	1698 (1773)	1650 (1627)	1631 (1644)	1593 (1601)
	5	C-C stretch + C-H wag	1690 (1677)	1576 (1603)	1565 (1553)	1507
	6	C-C stretch + C-H wag	1508	1444	1483	1436
	7	C-C stretch + C-H wag	1426 (1413)	1314 (1370)	1386 (1397)	1245 (1293)
	8	C-C stretch + C-H wag	1398	1397	1365	1341
	9	C-C stretch + C-H wag	1359 (1339)	1142 (1102)	1286 (1293)	1114
	10	C-C stretch + C-H wag	1240	1008	1203 (1191)	966
	11	C-C stretch	1139 (1135)	930 (926)	1110 (1100)	895
	12	ring deform	1006	867	981 (976)	835 (846)
	13	ring deform	819 (819)	772 (741)	795 (793)	740 (748)
	14	ring breathing	556 (562)	539 (528)	540 (547)	519 (515)
	15	ring deform	441 (438)	418 (401)	428 (424)	402 (401)
	16	ring deform	349 (361)	348 (337)	347 (350)	333 (331)
b_{1g}	17	C-H stretch	3210	2397	3121	2311
	18	C-H stretch	3188	2383	3090	2288
	19	C-H stretch	3170	2357	3073	2268
	20	C-C stretch + C-H wag	1738	1725	1594	1574
	21	C-C stretch + C-H wag	1594	1549	1563	1505
	22	C-C stretch + C-H wag	1531	1442	1459	1337
	23	C-C stretch + C-H wag	1363	1294	1314	1259
	24	C-C stretch + C-H wag	1255	1064	1219	1015
	25	C-C stretch + C-H wag	1242	1083	1167	1085
	26	C-C stretch + C-H wag	1159	937	1124	890
	27	ring deform	1021	872	1058	850
	28	ring deform	986	865	944	831
	29	ring deform	643	630	614	597
	30	ring deform	552	534	525	503
	31	ring deform	367	358	360	348
b_{2g}	32	oop C-C bend C-H wag	1047	869	996	814
	33	oop C-C bend C-H wag	964	782	877	702
	34	oop C-C bend C-H wag	804	630	747	592
	35	oop C-C bend	656	573	581	496
	36	oop ring deform	447	415	374	345
	37	oop ring deform	216	199	189	173
b_{3g}	38	oop C-C bend + C-H wag	1052	881	998	822
	39	oop C-C bend + C-H wag	972	840	909	767
	40	oop C-C bend + C-H wag	865	808	779	722
	41	oop C-C bend	782	659	701	591
	42	oop C-C bend	681	617	606	555
	43	oop C-C bend	472	417	473	415
	44	oop ring deform	310	293	276	260
	45	oop ring deform	126	115	135	122

TABLE 5. (*continued*).

Symmetry	Number	Vibration type	$S_0\ ^1A_g$				$S_1\ ^1B_{2u}$			
			h_{12}		d_{12}		h_{12}		d_{12}	
			Calc.[a]	(Obs.)[b]	Calc.[a]	(Obs.)[b]	Calc.[c]	(Obs.)[d]	Calc.[c]	(Obs.)[d]
a_u	46	oop C-C bend + C-H wag	1044		872		992		817	
	47	oop C-C bend + C-H wag	956		815		869		736	
	48	oop C-C bend + C-H wag	817		685		765		648	
	49	oop C-C bend	671		557		622		504	
	50	oop C-C bend	555		494		497		442	
	51	oop ring deform	251		226		228		203	
	52	oop ring torsion	12	(28)	11	(23)	44	(47)	42	(45)
b_{1u}	53	oop C-C bend + C-H wag	1055		884		1003		828	
	54	oop C-C bend + C-H wag	981		826		914		761	
	55	oop C-C bend + C-H wag	864		790		782		714	
	56	oop C-C bend	808		675		719		591	
	57	oop C-C bend	581		527		516		472	
	58	oop C-C bend	494		441		477		423	
	59	ring deform	183		171		173		160	
	60	butterfly	99	(107)	94	(101)	85	(96)	79	(91)
b_{2u}	61	C-H stretch	3210		2397		3121		2311	
	62	C-H stretch	3192		2385		3092		2290	
	63	C-H stretch	3172		2360		3076		2272	
	64	C-C stretch	1701		1664		1589		1513	
	65	C-C stretch	1693		1688		1563		1557	
	66	C-C stretch + C-H wag	1515		1422		1454		1343	
	67	C-C stretch + C-H wag	1447		1329		1397		1208	
	68	C-C stretch	1387		1366		1234		1279	
	69	C-C bend + C-H wag	1268		1089		1203		1046	
	70	C-C bend + C-H wag	1198		897		1148		859	
	71	C-C stretch + C-H wag	1123		914		1098		879	
	72	ring deform	840		803		795		759	
	73	ring deform	811		757		790		724	
	74	ring deform	603		580		563		536	
	75	ring deform	475		444		452		421	
b_{3u}	76	C-H stretch	3237		2410		3150		2325	
	77	C-H stretch	3190		2386		3091		2289	
	78	C-H stretch	3170		2358		3073		2268	
	79	C-C stretch + C-H wag	1718		1693		1573		1518	
	80	C-C stretch + C-H wag	1581		1555		1491		1387	
	81	C-C stretch + C-H wag	1559		1477		1375		1284	
	82	C-C stretch + C-H wag	1376		1303		1312		1209	
	83	C-C stretch + C-H wag	1322		1187		1232		1198	
	84	C-C stretch + C-H wag	1242		1072		1191		1010	
	85	C-C stretch + C-H wag	1179		1035		1139		947	
	86	ring deform + C-H wag	1146		871		1075		823	
	87	ring deform	1060		933		989		895	
	88	ring deform	797		757		753		714	
	89	ring deform	551		539		511		497	
	90	ring deform	258		244		245		231	

[a] Results of RHF/6-311+G(d,p) are scaled by 0.955.
[b] Determined using the dispersed fluorescence spectrum with an accuracy of ± 3 cm^{-1}.
[c] Results of RCIS/6-31+G(d,p) are scaled 0.918.
[d] Determined using the fluorescence excitation spectrum with an accuracy of ± 1 cm^{-1}.

Figure captions

Figure 1. Molecular structure and coordinate axes of perylene.

Figure 2. Fluorescence excitation spectra of $S_1\ ^1B_{2u} \leftarrow S_0\ ^1A_g$ transition of jet-cooled (a) perylene-h_{12} and (b) perylene-d_{12} (blue traces). Red traces indicate spectra at higher vibrational temperature with lower Ar gas pressure level.

Figure 3. Dispersed fluorescence spectra for excitations of $S_1\ ^1B_{2u} \leftarrow S_0\ ^1A_g\ 0_0^0$ bands of jet-cooled (a) perylene-h_{12} and (b) perylene-d_{12}.

Figure 4. Normal coordinates of four low frequency modes.

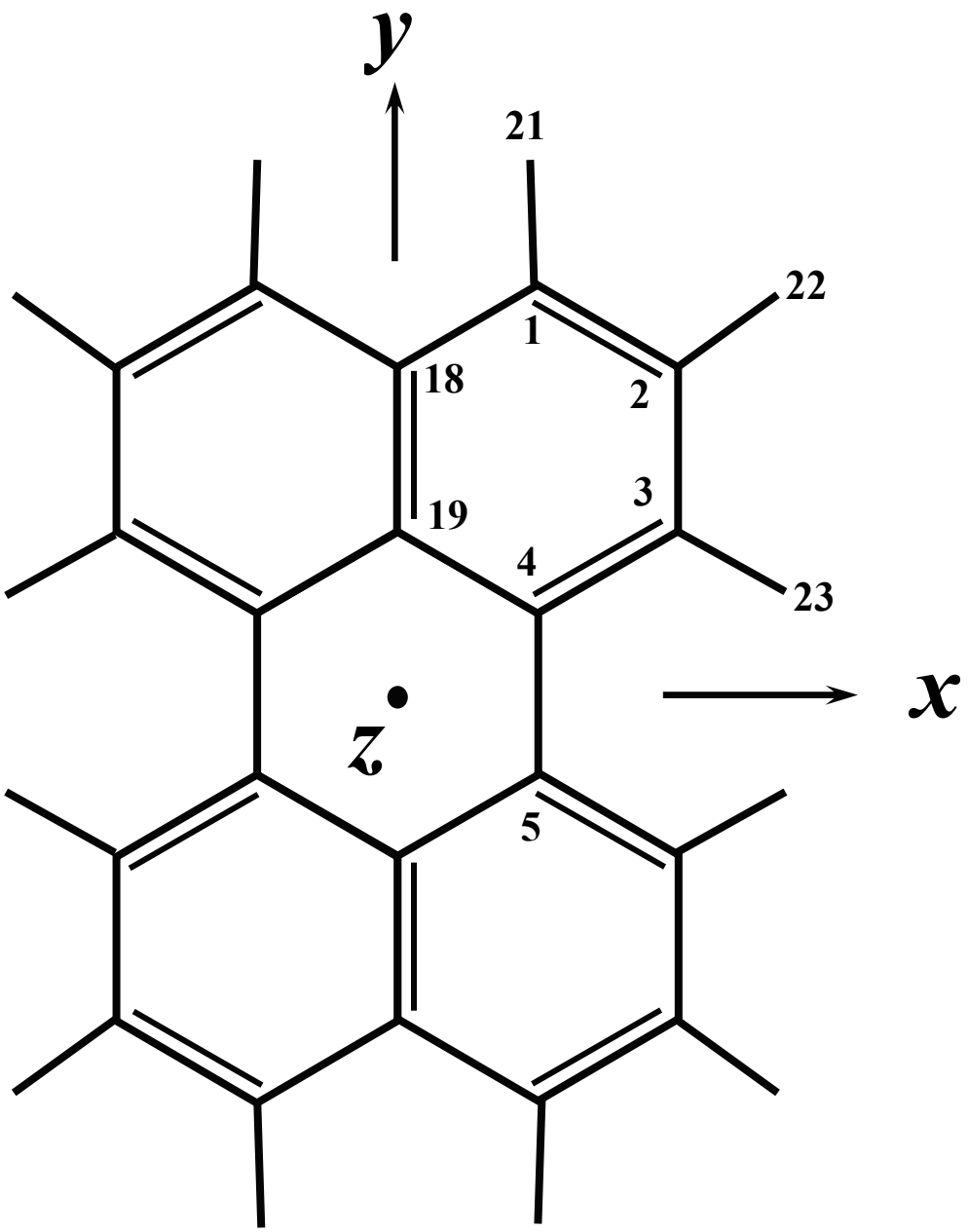

Figure 1. Y. Suganuma *et al.*

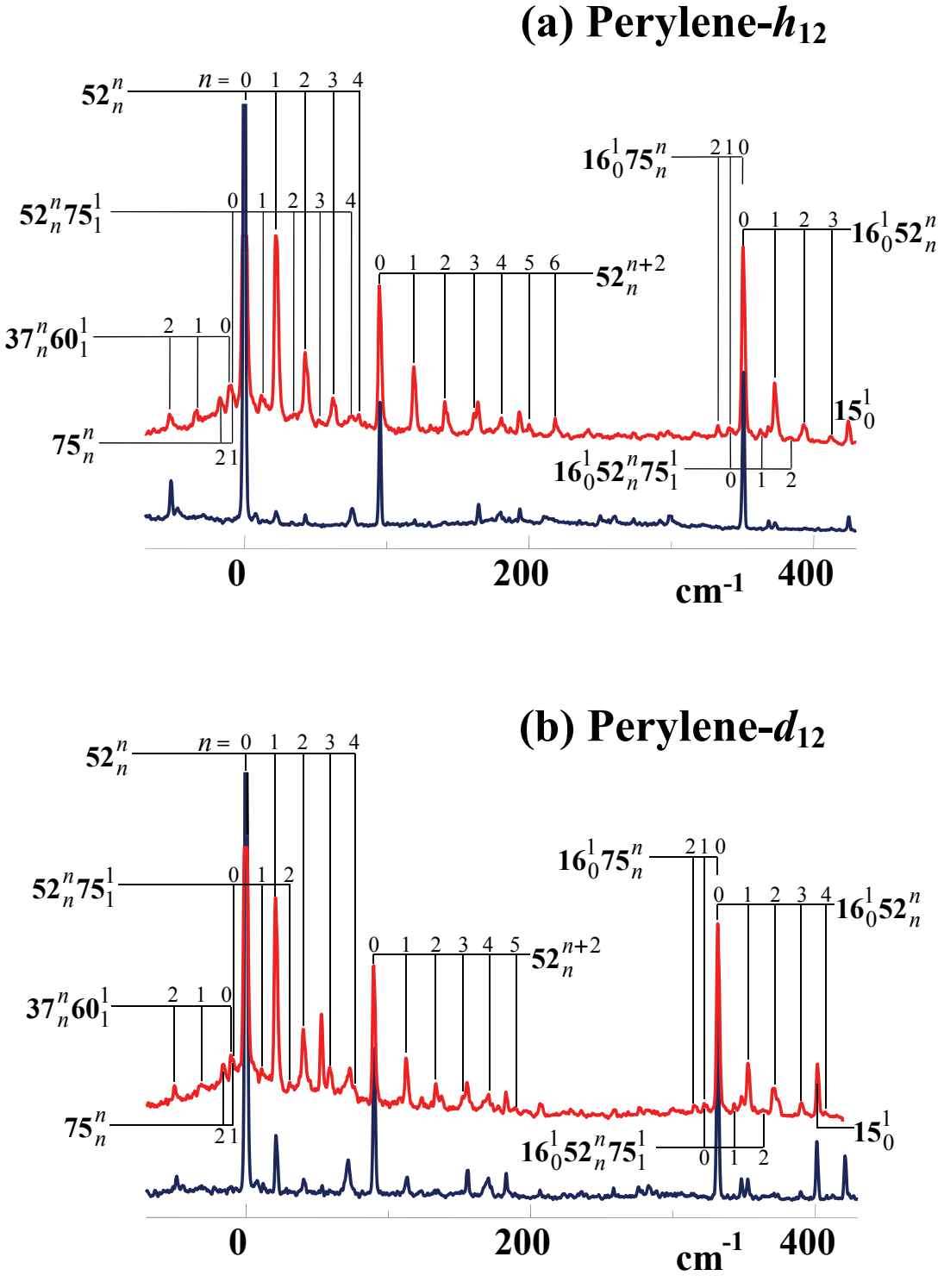

Figure 2. Y. Suganuma *et al.*

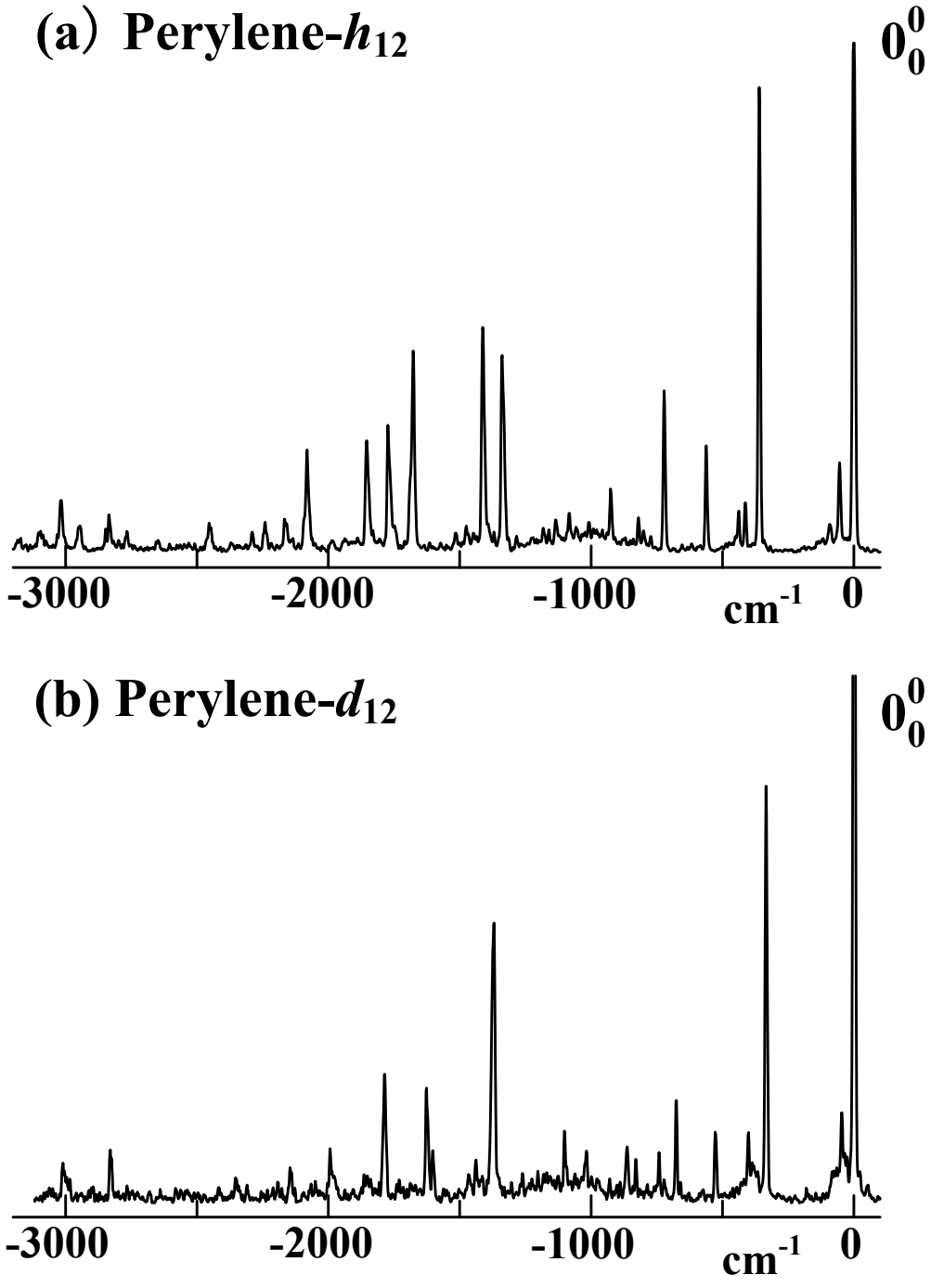

Figure 3. Y. Suganuma *et al*.

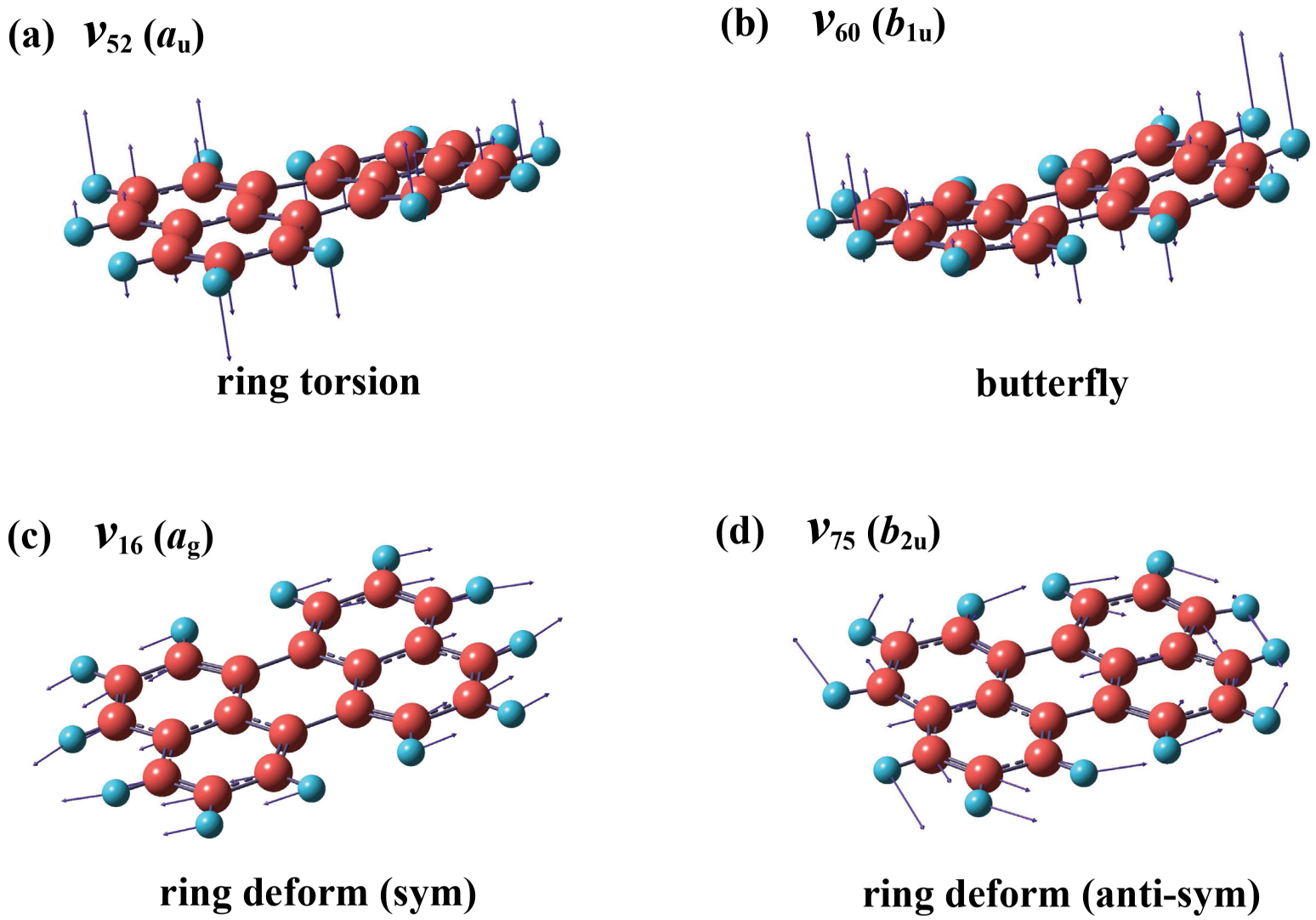

Fig.ure 4. Y. Suganuma *et al.*